Biomineralization

DOI: 10.1002/ange.201000679

Structural Control of Crystal Nuclei by an Eggshell Protein**

*Colin L. Freeman, John H. Harding, David Quigley, and P. Mark Rodger**

The use of biomolecules in nature to direct crystal growth leads to a degree of polymorph and morphology control that far surpasses anything currently accessible in a laboratory. Examples include the intricate nano- and microcrystalline structures found in mollusk shells,[1] coccoliths,[2] and eggshells,[3] which imbue the shells with important physical properties. Recent work has exploited biomolecules[4,5] and biomimetic processes[6,7] to fabricate new materials, but the scope for this would be greatly enhanced if the mechanism by which the biomolecules effect this control were better understood. Molecular simulation should be an ideal tool for identifying these mechanisms. Methods have been developed to model the clustering of inorganic ions on biomolecules,[8] but simulating the onset of long-range crystalline order in the inorganic deposit due to the biomolecule has not been possible. Crystal nucleation, a crucial step in polymorph selection, occurs on timescales that have hitherto been inaccessible to molecular simulation. Herein, we show that our recent developments to metadynamics,[9,10] coupled with the latest generation of leadership-class computing, have now made it possible to simulate the role of a native protein in controlling the onset of mineral crystallization. We illustrate this process with the first molecular simulation of spontaneous crystallization of amorphous $CaCO_3$ in the presence of the chicken eggshell protein ovocleidin-17 (OC-17).

Eggshells have an intricate structure that consists of two domains attached to an inner membrane.[11] The first domain is an array of small polycrystalline calcite clusters (mammillary caps) attached to the membrane that surrounds the albumin; the second domain (pallisade layer) consists of elongated calcite crystals with partial alignment. Experiments have identified various proteins associated with eggshell formation. One class, C-type lectin-type proteins, is found only within the mineral region and is important in controlling calcite deposition.[12] In vitro studies with OC-17 (chicken) and ansocalcin (goose) have shown that these proteins promote calcite formation and define the crystal morphology.[13–15]

[*] D. Quigley, Prof. P. M. Rodger
Department of Chemistry and Centre for Scientific Computing
University of Warwick
Coventry, CV4 7AL (UK)
E-mail: p.m.rodger@warwick.ac.uk
C. L. Freeman, J. H. Harding
Department of Engineering Materials, University of Sheffield
Sheffield, S1 3JD (UK)

[**] We wish to thank the EPSRC for support under grants GR/S80103, GR/S80127, and EP/F055471/1, and Martyn Foster (Cray Research Ltd) and Ilian Todorov (Daresbury Laboratory) for help in adapting codes to HECToR. All authors contributed equally to this work.

Supporting information for this article is available on the WWW under http://dx.doi.org/10.1002/anie.201000679.

There is now much experimental evidence that many biominerals,[16] including eggshells,[17] begin as nanoparticle deposits of an amorphous inorganic material. Our recent simulations[10] support this, showing amorphous calcium carbonate (ACC) to be energetically stable, even at larger particle sizes where calcite becomes thermodynamically preferred. The interaction between OC-17 and ACC particles of various sizes is therefore likely to be fundamental to the mechanism by which OC-17 controls calcite growth, and so forms the focus of the work described herein.

Simulations[18] were performed using metadynamics (metaD).[19,20] MetaD extends conventional molecular dynamics (MD) to sample the free-energy landscape in terms of collective coordinates (that is, order parameters or reaction coordinates). It is particularly good at finding the rare transitions between different states of order. For most applications, one or two order parameters have proved sufficient, but we have found that for $CaCO_3$ we need to explore a six-dimensional landscape, with the parameters describing the local coordination geometry of the atoms and ions and the energetics of the $CaCO_3$ particle.[10,20] Simulations were performed on a molecule of OC-17 adsorbed onto an ACC nanoparticle and immersed in explicit water. Potentials were those of Freeman et al.[21] The protein configuration was taken from the crystal structure.[13] Two different sizes of nanoparticle (192 and 300 $CaCO_3$ formula units) were adopted from our earlier study without protein.[10] For both sizes, calcite is thermodynamically stable, whereas ACC is metastable with a free energy barrier of about 350 kJ mol^{-1}. Conventional MD was used to explore possible protein–particle binding geometries. Four configurations were selected from the trajectories for each nanoparticle: the three with lowest potential energy and the one with greatest protein/nanoparticle contact area. Each configuration was solvated and used to initiate metaD simulations. Calculations were performed on the UK national supercomputer;[22] each metaD simulation used 2048 processor cores for over 500 h. In total, the results reported herein expended five million core hours. During each metaD simulation, at least 8–12 spontaneous crystallization/re-amorphization events were observed, along with a wide range of nanoparticle morphologies. No previous molecular simulation has observed the spontaneous emergence of crystallinity in the presence of a protein.

Figure 1 shows a typical example of the binding motifs for the smaller nanoparticle. The protein bound most readily to the nanoparticle surface through two clusters of arginine residues, located on two loops of the protein and creating a "clamp" to the nanoparticle.

Free-energy hypersurfaces were obtained from the metaD simulations. Typical two-dimensional projections for the smaller particle are given in Figure 2. Two main minima are

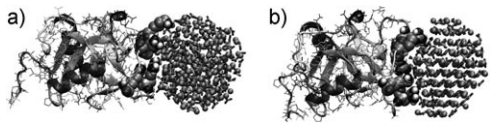

Figure 1. Ovocleidin-17 bound to an amorphous (a) and a crystallized (b) calcium carbonate nanoparticle containing 192 formula units. The highlighted residues depicted as overlapping spheres are those that remain in contact with the surface over the entire simulation trajectory (ARG81, ARG86; and LYS106, ARG108, ARG109) and are located on two loops. (See Supporting Information, Figure S1 for color.)

apparent for the nanoparticle in the absence of OC-17, which correspond to the ACC phase and calcite. There is also a third, smaller, minimum with a structure similar to vaterite. The calcite basin is more stable than ACC (by about 250 kJ mol^{-1}), but with a large free energy barrier (ca. 350 kJ mol^{-1}), ensuring the amorphous state is long-lived. In the presence of OC-17, bound through the arginine clusters (Figure 1), the topography of this free-energy landscape changes dramatically: the barrier stabilizing the amorphous phase disappears, as does the intermediate basin. Thus, the presence of OC-17 catalyzes the transformation of the ACC nanoparticle into a calcite crystallite.

With the larger nanoparticle (300 formula units), binding sites were mediated through the same arginine residue clamp identified for the smaller particle, but the binding was weaker. In the eight simulations we performed, the protein never desorbed from the smaller nanoparticle, but always desorbed from the larger one. In each case, desorption occurred at or after nucleation of calcite (Supporting Information, Figure S6). These results suggest that the clamping mechanism was ineffective with the larger calcite nanoparticle, and the change in the shape or structure of the nanoparticle consequent on the amorphous–crystalline transition was enough to dislodge the protein. To probe this effect further, conventional MD simulations were performed on both nanoparticles with OC-17 bound in a geometry matched to the optimal geometry found from the smaller nanoparticle metaD simulations. The smaller nanoparticle deformed under the influence of the protein (Figure 3), optimizing the protein–$CaCO_3$ interactions. With more ions, however, the influence of the protein no longer dominated over intra-mineral interactions, so that the larger particle retained its shape with a curvature that gave limited contact with the protein. We conclude that the lower curvature of the larger nanoparticle diminished the strength of the protein–nanoparticle binding.

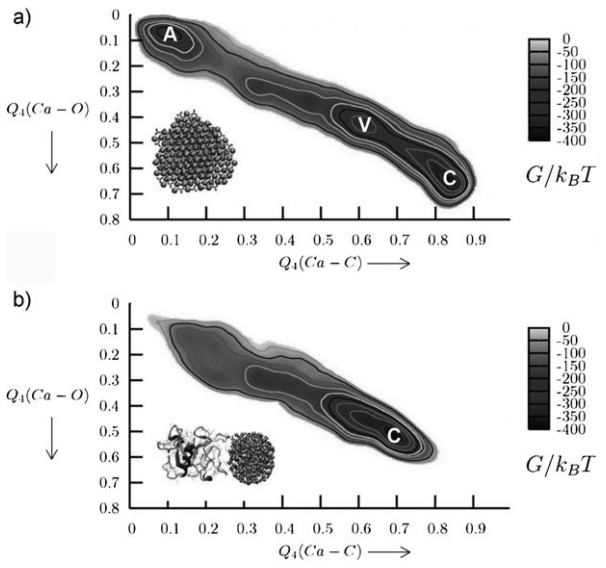

Figure 2. Projections of Gibbs free energy maps for a nanoparticle containing 192 units of $CaCO_3$. a) Nanoparticle in water, b) nanoparticle with OC-17 bound in water. The order parameters used for the axes measure symmetry in the arrangement of the carbon or oxygen atoms around the calcium ions. The letters label minima where local order is associated with a macroscopic polymorph: A = ACC, C = calcite, V = vaterite-like. Further details can be found in Ref. [10]. (See Supporting Information, Figure S2 for color.)

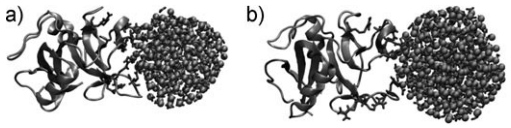

Figure 3. Influence of nanoparticle size on binding action of ovocleidin-17 to amorphous calcium carbonate nanoparticles. With 192 formula units (a), the particle shape allows four residues to bind to the surface, and there is some evidence of distortion of the particle to accommodate the protein even in normal MD simulations. For 300 formula units (b), the surface curvature of the nanoparticle is too small to allow contact with the inner residues and binding occurs through just a single residue on each loop; no significant distortion of this larger nanoparticle towards the protein is observed. (See Supporting Information, Figure S3 for color.)

It is known that OC-17 modifies crystal morphology. As this is normally attributed to surface binding, the size-dependent desorption noted above is intriguing. The surfaces involved in morphological binding, however, do not show nanoscale curvature. We therefore ran MD simulations of OC-17 on planar, stepped, and amorphous $CaCO_3$ surfaces. Strong binding to the crystalline surfaces was observed, but the presence of a tightly bound surface water layer led to a different binding motif. Extended arginine groups penetrated the water layer and provided points of strong attachment with minimal disruption to the surface water layer (Figure 4). Protein conformations that maximized calcite–protein contact by excluding water invariably gave weaker binding energies. No structured water layer was found at the amorphous surface, and in this case the strongest binding geometry was one that excluded surface water, with 13 amino acids in contact with the surface. The structure of the water layer around calcite nanoparticles is much closer to that above the amorphous surface than the crystalline surfaces.[23] Therefore, the binding of OC-17 to nanoparticles is dominated by optimal contacts between the charged residues (mainly arginine) and the $CaCO_3$, whilst its recognition of planar crystal surfaces is mediated by compatibility with structured surface water.

In summary, we have presented the first molecular simulations of mineral crystallization under protein control. Using metadynamics in conjunction with leadership-class computing, we were able to simulate about 50 separate, spontaneous transitions between polymorphs in a $CaCO_3$ nanoparticle. The results show that the chicken eggshell

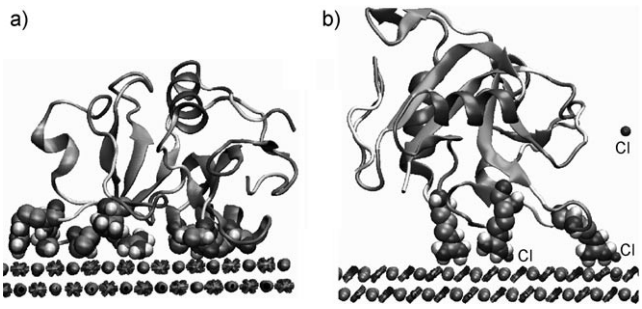

Figure 4. Two binding configurations of protein to the calcite (10.4) surface. The residues that bind to the surface are depicted as overlapping spheres. Binding energies: a) (-53 ± 42) kJ mol^{-1}, b) (-422 ± 43) kJ mol^{-1}. The residues bound to the surface are a) SER 27, 31 and 85; ARG 28, 34, 35, 86, 89 and 112; and ALA 83; b) ARG 46, 86 and 89. The binding energy is much lower for the configuration with fewer ARG in contact with the surface, demonstrating the importance of minimizing the disruption of the structured surface water. (See Supporting Information, Figure S4 for color.)

protein ovocleidin-17 can facilitate a transition from amorphous particle to calcite crystal. Intriguingly, strong binding was observed only with smaller nanoparticles (192 formula units); with a larger particle size (300 formula units) the protein consistently desorbed from the calcite phase. Strong binding is regained for very large crystalline surfaces, but in this case mediated by structured surface water. Whilst computational resources prevent a more detailed exploration of different particles sizes, the results lead us to propose that OC-17 acts as a catalyst by binding to amorphous calcium carbonate nanoparticles, transforming them to calcite nuclei, and then desorbing as the calcite begins to grow, thus leaving the OC-17 available to bind to another ACC nanoparticle (see Figure 5). This catalytic cycle provides a mechanism for forming the polycrystalline mammillary caps that are deposited on the organic membrane as the first stage of eggshell formation.

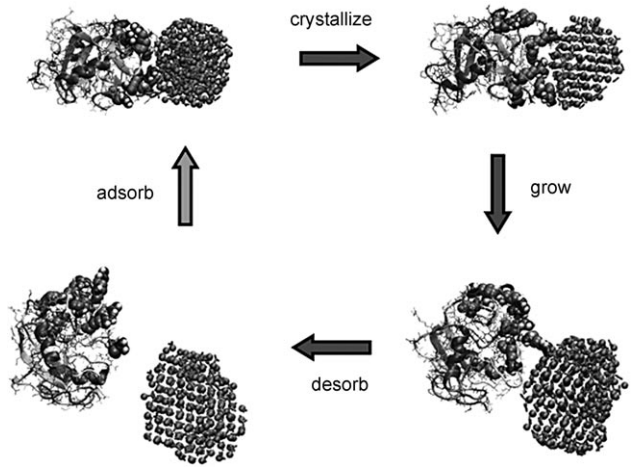

Figure 5. The ovocleidin-17 (O-17) catalytic cycle. OC-17 binds to a small amorphous calcium carbonate (ACC) nanoparticle and induces the nanoparticle to crystallize as calcite; the calcite begins to grow, causing the desorption of the OC-17 and making it available to bind to another ACC nanoparticle. This process enables rapid formation of many calcite crystals, as required for the polycrystalline mammillary layer. (See Supporting Information, Figure S5 for color.)

Received: February 4, 2010
Published online: June 9, 2010

Keywords: biomineralization · crystal growth · molecular dynamics · nanoparticles

[1] a) F. Marin, G. Luquet, B. Marie, D. Medakovic, *Curr. Top. Dev. Biol.* **2007**, *80*, 209; b) B. Marie, G. Luquet, J. P. P. De Barros, N. Guichard, S. Morel, G. Alcaraz, L. Bollache, F. Marin, *FEBS J.* **2007**, *274*, 2933; c) F. Nudelman, H. H. Chen, H. A. Goldberg, S. Weiner, L. Addadi, *Faraday Discuss.* **2007**, *136*, 9.
[2] a) N. Ozaki, S. Sakuda, H. Nagasawa, *Biochem. Biophys. Res. Commun.* **2007**, *357*, 1172; b) K. Henriksen, J. R. Young, P. R. Bown, S. L. S. Stipp, *Palaeontology* **2004**, *47*, 725.
[3] R. Lakshminarayanan, R. M. Kini, S. Valiyaveettil, *Proc. Natl. Acad. Sci. USA* **2002**, *99*, 5155.
[4] N. Nuraje, S. Mohammed, L. L. Yang, H. Matsui, *Angew. Chem.* **2009**, *121*, 2584; *Angew. Chem. Int. Ed.* **2009**, *48*, 2546.
[5] Y. X. Huang, J. Buder, R. Cardoso-Gil, Y. Prots, W. Carrillo-Cabrera, P. Simon, R. Kniep, *Angew. Chem.* **2008**, *120*, 8404; *Angew. Chem. Int. Ed.* **2008**, *47*, 8280.
[6] C. Li, L. M. Qi, *Angew. Chem.* **2008**, *120*, 2422; . *Chem. Int. Ed.* **2008**, *47*, 2388.
[7] H. Tlatlik, P. Simon, A. Kawska, D. Zahn, R. Kniep, *Angew. Chem.* **2006**, *118*, 1939; *Angew. Chem. Int. Ed.* **2006**, *45*, 1905.
[8] A. Kawska, O. Hochrein, J. Brickmann, R. Kniep, D. Zahn, *Angew. Chem.* **2008**, *120*, 5060; *Angew. Chem. Int. Ed.* **2008**, *47*, 4982.
[9] D. Quigley, P. M. Rodger, *J. Chem. Phys.* **2008**, *128*, 154518.
[10] D. Quigley, P. M. Rodger, *J. Chem. Phys.* **2008**, *128*, 221101.
[11] Y.-C. Chien, M. T. Hincke, H. Vali, M. D. McKee, *J. Struct. Biol.* **2008**, *163*, 84.
[12] a) K. Mann, F. Siedler, *Comp. Biochem. Physiol. Part B* **2006**, *143*, 160; b) K. Mann, *Br. Poult. Sci.* **2004**, *45*, 483.
[13] J. P. Reyes-Grajeda, A. Moreno, A. Romero, *J. Biol. Chem.* **2004**, *279*, 40876.
[14] R. Lakshminarayanan, J. S. Joseph, R. M. Kini, S. Valiyaveettil, *Biomacromolecules* **2005**, *6*, 741.
[15] R. Lakshminarayanan, X. J. Loh, S. Gayathri, S. Sindhu, Y. Banerjee, R. M. Kini, S. Valiyaveettil, *Biomacromolecules* **2006**, *7*, 3202.
[16] a) Y. Ma, S. Weiner, L. Addadi, *Adv. Funct. Mater.* **2007**, *17*, 2693; K. Benzerara, N. Menguy, P. Lopez-Garcia, T. H. Yoon, J. Kazmierczak, T. Tyliszczak, F. Guyot, G. E. Brown, *Proc. Natl. Acad. Sci. USA* **2006**, *103*, 9440; b) Y. Politi, T. Arad, E. Klein, S. Weiner, L. Addadi, *Science* **2004**, *306*, 1161; c) L. Addadi, S. Raz, S. Weiner, *Adv. Mater.* **2003**, *15*, 959.
[17] S. Gayathri, R. Lakshminarayanan, J. C. Weaver, D. E. Morse, R. M. Kini, S. Valiyaveettil, *Chem. Eur. J.* **2007**, *13*, 3262.
[18] Methods for the molecular dynamics and metadynamics simulations are given in the Supporting Information.
[19] A. Laio, M. Parrinello, *Proc. Natl. Acad. Sci. USA* **2002**, *99*, 12562.
[20] D. Quigley, P. M. Rodger, *Mol. Simul.* **2009**, *35*, 613.
[21] C. L. Freeman, J. H. Harding, D. J. Cooke, J. A. Elliott, J. S. Lardge, D. M. Duffy, *J. Phys. Chem. C* **2007**, *111*, 11943.
[22] HECToR; at the time it ranked 20th in the world top 500 list.
[23] D. Cooke, J. A. Elliot, *J. Chem. Phys.* **2007**, *127*, 104706.